Ultrasonics Sonochemistry 93 (2023) 106292

Contents lists available at ScienceDirect

Ultrasonics Sonochemistry

journal homepage: www.elsevier.com/locate/ultson

Covalent binding of ultrasound-treated japonica rice bran protein to catechin: Structural and functional properties of the complex

Yanfei Guo [a], Minghao Wang [a], Kaiwen Xing [a], Mingzhe Pan [a,*], Liqi Wang [b]

[a] School of Food Science, Northeast Agricultural University, Harbin 150030, China
[b] School of Food Science, Harbin University of Commerce, Harbin 150000, China

ARTICLE INFO

Keywords:
Japonica rice bran protein
Catechins
Ultrasound treatment
Covalent bonding
Functional properties

ABSTRACT

Due to the existence of many disulfide bonds in japonica rice bran protein (JRBP) molecules, their solubility is poor, which seriously affects other functional properties. To improve the functional characteristics of JRBP molecules, they were processed by ultrasound technology, and JRBP-catechin (CC) covalent complex was prepared. The structural and functional properties of indica and japonica rice bran proteins and their complexes were compared; furthermore, the changes in the structural and functional properties of JRBP-CC under different ultrasound conditions were investigated. The results showed that compared with indica rice bran protein (IRBP), the secondary structure of JRBP-CC was very different, the water holding capacity (WHC) was higher, and the emulsification performance was better. Different ultrasound conditions had different effects on the functional properties of JRBP-CC. When the ultrasound power was 200 W, the λ_{max} redshift of the JRBP-CC complex was the most significant, the particle size was the smallest, the absolute value of the zeta potential was the largest, and the hydrophobicity and microstructure of the JRBP-CC complex were the best. Concurrently, the maximum WHC and oil holding capacity (OHC) of JRBP-CC under these conditions were 7.54 g/g and 6.87 g/g, respectively. Moreover, the emulsifying activity index (EAI) and emulsifying stability index (ESI) were 210 m^2/g and 47.8 min, respectively, and the scavenging activities of 1,1-diphenyl-2-picrylhydrazyl (DPPH) and $ABTS^+$ were 71.96 % and 80.07 %, respectively.

1. Introduction

Rice, as one of the most important food crops worldwide, contains abundant nutrients [1]. In China, rice is usually divided into two subspecies: japonica and indica rice [2]. Compared with indica rice, japonica rice is mainly planted in northeastern China and has the advantage of greater viscosity [3]. Although the protein content in japonica rice is lower than that of other common cereals (such as wheat, jade rice, wheat, and millet), japonica rice protein is rich in nutrients, has a reasonable ratio of amino acids, and its lysine and methionine content is higher than that of other grain proteins, so it has a high biological effect. In addition, it is a low antigenic protein which is not likely to produce allergic reactions [4]. Japonica rice bran is an underutilized by-product of japonica rice milling, which is nutritious and rich in protein, fat, carbohydrates, and other components [5–7]. Japonica rice bran protein (JRBP) is rich in albumin, globulin, glutelin and prolamin [8], and the content of gluten is higher than that of indica rice [9]. JRBP is a fully valent protein containing 18 amino acids and eight essential amino acids, rich in nutrients, and can be used as a hypoallergenic food ingredient in infant formula [10]. JRBP contains many disulfide bonds, which causes poor solubility and greatly affects other functional characteristics, especially emulsifying properties and foaming characteristics, limiting the application of native JRBP in processing. Therefore, the spatial structure of protein molecules is often modulated by various methods to change the intramolecular structure and binding mode of the protein to improve its functional properties.

Currently, ultrasound treatment emerges as a new type of protein modification method, with a frequency and intensity ranging between 20 and 100 kHz and 10–1000 W/cm^2, respectively [11]. Ultrasound modifies the molecular structure and spatial conformation of proteins due to unique cavitation and microstreaming currents [12]. When ultrasonic waves propagate in aqueous media, the rupture of gas bubbles in the system generates high temperature (5000 K) and high pressure (50 MPa, 3×10^{-4}) in a short time [13]. At this time, mechanical shear, heating, dynamic agitation, intense shear forces, and turbulence will further process the protein, thereby changing its structure and

* Corresponding author.
E-mail address: gyfgbo@126.com (M. Pan).

https://doi.org/10.1016/j.ultsonch.2023.106292
Received 17 October 2022; Received in revised form 25 December 2022; Accepted 5 January 2023
Available online 12 January 2023

properties [14]. Studies have shown that ultrasound treatment of protein can reduce particle size and improve its solubility and emulsifiability [15]. The study by Sun et al. [16] demonstrated that ultrasound treatment improved the solubility, emulsifying properties, and stability of rice bran protein. A similar conclusion appeared in the study of Wang et al. [17], where the structure of JRBP was changed by the combined treatment of ultrasound and chlorogenic acid to obtain a complex with good functional properties to broaden its application in food processing emulsifiers. Therefore, ultrasound is considered to be a safe and effective food processing technology that can be applied to protein modification.

Polyphenols, the main group of antioxidants, are aromatic compounds in which at least one hydrogen of the aromatic hydrocarbon ring is replaced by a hydroxyl group (–OH). The interaction between proteins and polyphenols can modify their structural and functional properties [18]. The covalent interaction of polyphenols with proteins refers to the oxidation of phenolic compounds under alkaline conditions to form the corresponding quinones, and then undergo a nucleophilic addition reaction with the nucleophilic groups in the protein (such as amino, thiol, or certain amino acid residues) to form covalent complexes [19]. In the study of Karefyllakis et al. [20], the establishment of covalent binding between sunflower protein isolate and chlorogenic acid at pH 9 increased the polarity of the interfacial binding site, leading to a decrease in the hydrophobicity of the protein surface. Catechin (CC) is a type of flavonoid widely found in plants such as tea. Its antioxidant capacity is higher than that of other antioxidants such as butylated hydroxyanisole (BHA), butylated hydroxytoluene (BHT), alpha-tocopherol, vitamin E, and other plant extracts [21]. Binding of CC to protein can improve the solubility, thermal stability, oxidative stability, and emulsification properties of the complexes [22]. For example, Tian et al. [23] studied that the binding of CC with sodium caseolate to obtain protein–polyphenol complexes with improved physical and oxidative stability.

In this study, JRBP was treated with ultrasound and JRBP-CC complexes were prepared to investigate the effects of ultrasound on the structural and functional properties of JRBP and its complexes. The JRBP treated at different ultrasound strengths was covalently bound to CC, and the effects of ultrasound treatment on the secondary structure and sulfhydryl content of JRBP and its complexes were discussed. We expect that ultrasound treatment improves the water-holding capacity (WHC), oil holding capacity (OHC), emulsifying properties, and oxidative stability of JRBP-CC complexes. This provides a theoretical basis for the application of polyphenol-protein covalent complexes in emulsifiers, broadens their application in the food processing industry, and promotes economic and social benefits.

2. Materials and methods

2.1. Materials

Japonica rice bran powder was purchased from Xingwang Rice Bran Oil Co., ltd. (Liaoning, China). CC (≥90 %) was purchased from Nanjing Dulai Biotechnology Co., ltd. Additionally, 1,1-diphenyl-2-picrylhydrazyl (DPPH) was purchased from Shanghai Ika Biotechnology Co., ltd. All other reagents were of analytical grade.

2.2. Preparation of JRBP

Defatted rice bran was mixed thoroughly with five volumes of distilled water, and then adjusted to pH 8 with 1 mol/L NaOH. The mixture was stirred for 30 min at room temperature and then centrifuged at 5000 rpm and 4 °C for 30 min. The supernatant containing the protein was collected and adjusted to pH 4.5 with 1 mol/L HCl, and the protein was collected by centrifugation at 5000 rpm and 4 °C for 30 min. The precipitate was washed with water and the pH value was adjusted to 7.0. The samples were lyophilized to obtain JRBP.

2.3. Ultrasound treatment of JRBP

JRBP was dissolved in phosphate buffer (0.01 mol/L, pH 7.0) at a ratio of 1:25 (m/v), and then poured into a 250 mL beaker. Ultrasound treatment was performed following the study of Wang et al [24]. The beaker with the JRBP solution was placed in ice water to maintain a temperature below 20 °C. Furthermore, the solution was treated using an ultrasonic generator. At an ultrasound frequency of 20 kHz, different ultrasound powers (0, 100, 200, 300, and 400 W) were selected for ultrasound treatment for 10 min, and the ultrasonic pulse system was set to operate for 2 s and rest for 2 s.

2.4. Preparation of JRBP-CC

The JRBP-CC complex was prepared according to the method of Sui et al [25]. JRBP was dissolved in phosphate buffer and the pH was adjusted to 9.0. CC (0.15 %, w/v) was dissolved in the protein solution separately and the pH was adjusted to 7.0 after stirring for 24 h at 25 °C. JRBP-CCs were obtained and freeze-dried. The sample treatment is shown in Table 1.

2.5. Sulfhydryl (SH) content analysis

The sulfhydryl content of JRBP was measured by Ellman's reagent method [26]. Samples were mixed with Ellman's reagent at 25 °C for a certain time. The absorbance of the sample was measured at 412 nm.

2.6. Fourier transform infrared spectroscopy (FTIR)

Infrared spectra were determined using a Fourier Transform Infrared spectrometer at a temperature of 25 °C. The scan range was set from 450 to 4000 cm^{-1}, the resolution was 4 cm^{-1}, and 64 scans were performed. Peak fitting software version 4.12 was used to calculate the relative amounts of secondary structures in the proteins.

2.7. Determination of fluorescence spectra

The sample solution was diluted with distilled water to a protein concentration of 0.2 mg/mL. The excitation wavelength was set at 295 nm and the emission wavelength range was set at 300–500 nm. The scanning speed was 600 nm/min and the slit width was 5 nm. Fluorescence emission spectra were measured at 20 °C with distilled water as blank.

2.8. Particle size / potential determination

The sample solution was diluted with distilled water to a protein concentration of 2 mg/mL. The refractive indices of protein and water were set at 1.46 and 1.33, respectively. Particle size was measured with a laser diffraction particle size analyzer. After calibrating the instrument for 2 min, the Zetasizer Nano ZSP particle size analyzer was used to measure the zeta potential.

2.9. Confocal laser scanning microscopy (CLSM)

A confocal laser scanning microscope was used to study the

Table 1
The samples of different ultrasonic treatment conditions.

	Native	A	B	C	D	E
Sample	0 W JRBP	0 W JRBP-CC	100 W JRBP-CC	200 W JRBP-CC	300 W JRBP-CC	400 W JRBP-CC

Note: The JRBP indicates Japonica rice bran protein, and the CC indicates catechin.

microstructure of the samples. The samples were diluted following the method of Geremias-Andrade et al. [27]. Briefly, 1 mL of diluted sample was mixed with 40 μL of Nile Blue solution and stained for 30 min. The samples were observed with a confocal laser scanning microscope (Leica Microsystems, Heidelberg GmbH, Germany).

2.10. Water holding capacity (WHC) and oil holding capacity (OHC)

WHC quantification was performed using the techniques reported by Li et al. [28]. A 0.20 g protein sample was placed in a centrifuge tube and weighed, then added into 5 mL of deionized water and mixed thoroughly to obtain the protein sample emulsion. The protein emulsion was allowed to stand for 24 h at room temperature and centrifuged at 3000*g* for 15 min. The supernatant was discarded and then the total mass of the centrifuge tube and the residue were weighed. The WHC formula was as follows:

$$\mathrm{WHC} = \frac{w_2 - w_1}{w_0} \times 100\%$$

where w_0 is the weight of the protein sample, g; w_1 is the weight of the tube and protein sample, g; and w_2 is the weight of the tube and residue, g.

OHC was determined according to the method of Zhu et al. [29]. A 0.10 g protein sample was placed in a centrifuge tube and weighed, then added into 4 mL of soybean oil and mixed thoroughly. The mixture was allowed to stand for 6 h at room temperature and then centrifuged at 2000*g* for 30 min. The supernatant was removed and the centrifuge tube was inverted for 20 min, and then the total mass of the tube and the residue were weighed. The OHC formula was as follows:

$$\mathrm{OHC} = \frac{W_2 - W_1}{W_0} \times 100\%$$

where W_0 is the weight of the protein sample, g; W_1 is the weight of the tube and protein sample, g; and W_2 is the weight of the tube and residue, g.

2.11. Analysis of emulsifying properties

The sample solution was prepared with phosphate buffer solution at a concentration of 10 μg/mL, and then corn oil (3:1, v/v) was added to prepare the emulsion and diluted 100 times with sodium dodecyl sulfate solution. The absorbance of the sample was measured at 500 nm. The emulsifying activity index (EAI) and emulsifying stability index (ESI) were calculated as follows:

$$EAI\left(m^2/g\right) = \frac{2 \times 2.303 \times A_0 \times D \times F}{10000 \times \theta \times L \times C}$$

$$ESI(\mathrm{min}) = \frac{A_0 \times (T_{10} - T_{10})}{A_0 - A_{10}}$$

where A_0 is the absorbance at 0 min, A_{10} is the absorbance at 10 min, C is the protein concentration (g/mL), D and F are the dilution factor (100), L is the optical path (1 cm), θ is the oil volume fraction (0.25), and T_{10}-T_0 is the time difference.

2.12. Measurement of the antioxidant activity of DPPH

DPPH free radical scavenging activity was determined according to the method of He et al. [30] with a slight modification. DPPH was dissolved in methanol and configured into a solution with a concentration of 10^{-4} mol/L, and then 2 mL of sample solution (0.5 mg/mL) was added into 2 mL of DPPH solution. The mixture was kept in darkness for 60 min, and the absorbance was measured at 517 nm using an ultraviolet (UV) spectrophotometer. The formula for determining the DPPH radical scavenging rate (%) was as follows:

$$DPPH\ radical\ scavenging\ rate\ (\%) = \frac{A_C - A_S}{A_C} \times 100\%$$

Where Ac is the absorbance of the DPPH working solution at 517 nm, and As is the absorbance of the DPPH and sample mixed solution at 517 nm.

2.13. Measurement of the antioxidant activity of $ABTS^+$

$ABTS^+$ scavenging activity was determined according to the method of Zhou et al. [31] with slight modifications. The 7 mM ABTS solution was mixed with 2.45 mM potassium persulfate solution at a ratio of 2:1 (v/v) and reacted at room temperature in the dark for 16 h. The $ABTS^+$ radical working solution was obtained by diluting the $ABTS^+$ solution with distilled water to an absorbance of 0.70 ± 0.02 at 734 nm. Moreover, 0.8 mL of $ABTS^+$ radical working solution was mixed with 200 μL of sample. The reaction was carried out at room temperature for 6 min, and then 200 μL of the mixed solution was transferred to the 96-well plate. The absorbance of the sample was measured at 734 nm using an enzyme label. The formula for the determination of the $ABTS^+$ radical scavenging rate (%) was as follows:

$$ABTS^+\ radical\ scavenging\ rate\ (\%) = \frac{A_0 - A}{A_0} \times 100\%$$

Where A_0 is the absorbance of the $ABTS^+$ free radical working solution at 734 nm, and A is the absorbance of the $ABTS^+$ free radical working solution and the mixed sample solution at 734 nm.

2.14. Statistical analysis

All experiments were performed at least three times and test data were analyzed using means and standard errors. Origin 2018 was used to record and analyze the data. Analysis of variance was performed using SPSS 26.0 with Duncan's test ($p < 0.05$).

3. Results and discussion

3.1. FTIR analysis

The secondary structures of the samples were analyzed by FTIR after ultrasound treatment. Amide I band was composed of bands corresponding to different secondary structures. The FTIR spectra of the samples are shown in Fig. 1(a). The interactions between JRBP and CC induced changes in the amide I compared with the control. This result revealed that the secondary structure of the samples was modified. In agreements with previous studies, the interaction between milk casein and tea polyphenols caused significant changes in the secondary structure [32]. With increasing ultrasound power, the amide I band changed to different degrees. When the ultrasound power was 200 W, the change in the amide I band was the most significant.

The amide I bands of the JRBP and JRBP-CC samples were fitted with the Gaussian area method, and the results are shown in Fig. 1(b). The contents of α-helix, β-sheet, β-turn, and random coil in the secondary structure of the JRBP-CC without ultrasound treatment were 18.95, 35.25, 20.18, and 23.74 %, respectively. Shi et al. prepared a rice bran protein catechin complex by combining indica rice bran protein (IRBP) with CC. Compared with the IRBP-CC complex prepared by Shi et al. [33], the JRBP-CC prepared in this study had a higher content of α-helix, β-sheet, and random coil, and a lower content of β-turn. The content of α-helix and β-sheet decreased with increasing ultrasound power, and the content of β-turn and random coil increased. When the ultrasound power was increased to 200 W, each secondary structure reached its maximum value. However, the trend changed when the power was too high (>200 W). These results showed that the molecular conformation of JRBP loosened during the ultrasound treatment, which agrees with the report

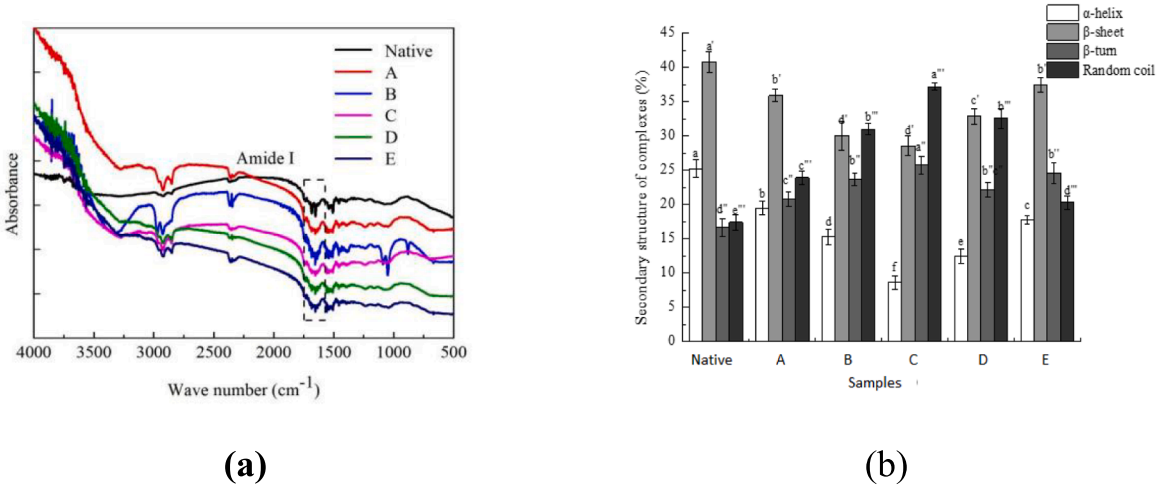

Fig. 1. FTIR analysis of JRBP and JRBP-CC complex under different ultrasonic conditions. (a) Fourier infrared spectrum. (b) Secondary structure content.

of Meng et al. [34]. This phenomenon occurs for two reasons: first, the introduction of CC caused the structure of JRBP to loosen, causing CC and JRBP to covalently bind. Second, after ultrasound treatment, the cavitation effect caused by bubble bursting made the protein structure loosen and stretch, so that the hydrophobic and polar groups inside the protein were exposed to the surface, and the degree of interaction between JRBP and CC increased.

3.2. Sulfhydryl content

As one of the important functional groups in proteins, sulfhydryl has high biological activity and plays an important role in the formation of gluten and gels [35]. The changes in the sulfhydryl content of JRBP and JRBP-CC were measured using an UV spectrophotometer, and the results are shown in Table 2. Compared with the control group, the introduction of CC reduced the content of sulfhydryl groups in JRBP. A significant effect of CC on the sulfhydryl content of JRBP through covalent interactions was observed. The decrease in sulfhydryl content was probably caused by their interaction with the hydroxyl groups of CC.

Furthermore, ultrasonication of the JRBP-CC complex also resulted in a decrease of sulfhydryl content within a certain extent. With increasing ultrasound power, the sulfhydryl content tended to decrease and then increase, and the increasing trend was not significant. The lowest value occurred at a power of 200 W. The effect of ultrasound treatment on the sulfhydryl content of the complexes can be explained by cavitation and mechanical shear [36]. The exchange reaction between –SH and disulfide bonds occurred readily within the JRBP molecule, leading to a decrease in the free –SH content. In the study of Ma et al. [37], it was found that the high intensity amplitude of ultrasound could change the sulfhydryl content of β-lactoglobulin by increasing the acoustic energy. When the power was above 200 W, the sulfhydryl group content in the JRBP-CC complex increased, but not significantly. This may be because the higher ultrasound power caused the JRBP structure to unfold and the hydrophobic amino acids to be exposed, which increased the hydrophobic group content. However, the higher ultrasound power promoted the covalent bonding of JRBP and CC to some extent, which resulted in the decrease of the hydrophobic group content. Therefore, although the sulfhydryl content increased, it was no significant difference [38]. Similar findings appear in the study of Rahman et al., in which high-power ultrasound treatment of soy protein was chosen, and this treatment exposed the buried sulfhydryl groups and increased the sulfhydryl content [39].

Table 2
Effect of ultrasonic power on the sulfhydryl content of JRBP and JRBP-CC under different ultrasonic conditions.

Sample	Sulfhydryl group ($\times 10^{-5}$ mol/g protein)
Native	10.0813 ± 0.38^{a}
A	1.5269 ± 0.41^{b}
B	1.1026 ± 0.22^{bc}
C	0.7456 ± 0.11^{c}
D	0.7658 ± 0.26^{c}
E	0.7747 ± 0.14^{c}

Note: The difference in letters indicates significant difference ($P < 0.05$).

3.3. Fluorescence spectrum analysis

Fluorescence spectroscopy is usually used to study the binding interaction between proteins and polyphenols, and can reflect the change in fluorescence intensity of tryptophan in proteins at the excitation wavelength of 280 nm. The fluorescence spectra of JRBP and its complex are shown in Fig. 2. As can be seen from Fig. 2, the λ_{max} of JRBP-CC was redshifted compared with that of JRBP, and the maximum fluorescence intensity was much lower than that of JRBP. This may be due to the interaction between JRBP and CC and the formation of a covalent bond in a covalent way.

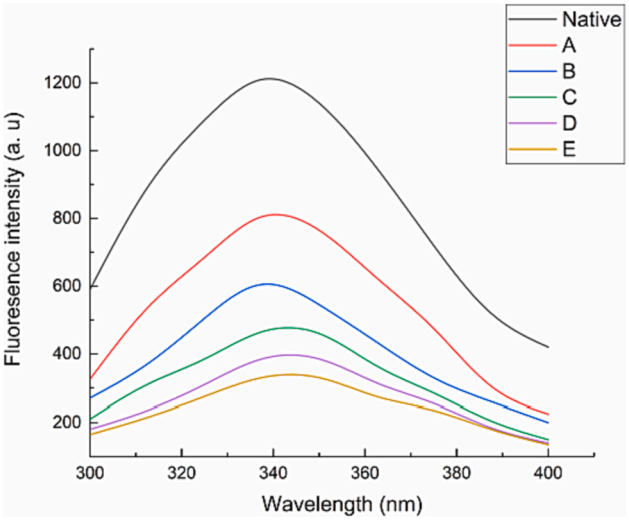

Fig. 2. Fluorescence spectra of JRBP and JRBP-CC complex under different ultrasonic conditions.

In addition, ultrasound treatment can make the λ_{max} of the complex exhibit different degrees of redshift. When the ultrasound power was 200 W, the redshift was the most significant. This may be because the ultrasound treatment unfolded the protein structure, the originally buried aromatic amino acid residues were exposed to the protein surface, and the polarity of the microenvironment was increased [40]. With the ultrasound power increasing from 0 W to 400 W, the maximum fluorescence intensity of JRBP-CC first increased and then decreased. When the ultrasound power was 200 W, the maximum fluorescence intensity was the lowest, which was similar to the study of Zhao et al. [41]. The reason for this phenomenon may be that the appropriate ultrasound treatment unfolded the protein structure. After the addition of CC, the binding of JRBP to CC caused the protein to form aggregates, and the originally exposed aromatic amino acids were buried again, which caused the fluorescence intensity to be reduced.

3.4. Particle size and zeta potential analysis

Particle size distribution usually reflects the degree of protein aggregation. The particle size distribution of the JRBP and JRBP-CC complex are shown in Fig. 3(a). As can be seen in Fig. 3(a), the particle size of JRBP and JRBP-CC without ultrasound treatment both exhibited double peaks, and the particle size of JRBP was smaller. This may be due to the unfolding of the internal structure of JRBP after the addition of CC, which covalently bound to the hydroxyl on the CC surface, thus increasing the particle size of the JRBP-CC complex. With increasing ultrasound power, the particle size of the complex first decreased and then increased with increasing ultrasound power. When the ultrasound power was 200 W, the particle size of the complex was the smallest and mainly concentrated at 7–100 nm. This may be because, after proper ultrasound treatment, the turbulence and shear caused by cavitation destroyed the spatial structure of the protein, aggravated the collision between molecules, and reduced the particle size.

The zeta potential usually reflects the charge density on the protein surface and the stability of the solution. The changes in the zeta potential of JRBP and its complexes are shown in Fig. 3(b). As can be seen in Fig. 3 (b), the absolute value of the zeta potential of JRBP was lower than that of the JRBP-CC complex without ultrasound treatment. This may be due to the covalent binding of JRBP and CC, which increased the electrostatic repulsion between ions and increased the absolute value of the zeta potential. With increasing ultrasound power, the absolute value of the zeta potential of the JRBP-CC complex first increased and then decreased. When the ultrasound power was 200 W, the absolute value of the zeta potential was the highest. The results indicated that an appropriate ultrasound treatment was beneficial to increase the absolute value of the zeta potential of the JRBP-CC complex to obtain better stability. This may be because ultrasound treatment unfolded the structure of JRBP, promoted the covalent bonding between JRBP and CC, caused the polar group to be exposed to the protein surface, and increased the charge [42].

3.5. CLSM observation

CLSM images of the JRBP and JRBP-CC complex are shown in Fig. 4. It can be seen that sample B, which was covalently bound to CC, was better dispersed compared to the untreated control. The JRBP-CC complex particles were inhomogeneous and the particle size increased after covalent bonding. Meanwhile, the dispersion of JRBP-CC particles improved with increasing ultrasound power of the treated complexes. The best results were presented at a treatment power of 200 W. Notably, at higher power (>200 W), the particles indicated a tendency to aggregate, which may be related to overtreatment. Overall, the ultrasound treatment resulted in a more uniform dispersion of the JRBP-CC complex in the solution system.

3.6. WHC and OHC analysis

The WHC and OHC values of JRBP-CC before and after ultrasound treatment by RPB are shown in Fig. 5(a). As can be seen in Fig. 5 (a), the WHC and OHC values of JRBP are 4.25 g/g and 1.82 g/g, respectively. Zhang et al. prepared IRBP by the co-precipitation method. Compared with the IRBP studied by Zhang et al. [43], the WHC content of the JRBP prepared in this study was higher and the OHC content was lower. A significant effect of different ultrasound powers on the WHC and OHC of the JRBP and JRBP-CC complexes was observed. With increasing ultrasound powers, the WHC and OHC of the JRBP-CC increased and then decreased. At an ultrasound power of 200 W, the WHC and OHC reached the maximum values of 7.54 g/g and 6.87 g/g, respectively. With increasing ultrasound power (>200 W), both WHC and OHC showed a decreasing trend. First, the addition of CC effectively enhanced the WHC and OHC of JRBP. Besides, the improvement of the WHC of the JRBP and JRBP-CC complexes can be attributed to the effect of ultrasonic waves on the molecular structure of proteins. The cavitation effect generated by the ultrasonic waves can promote the exposure of the polar amino acid

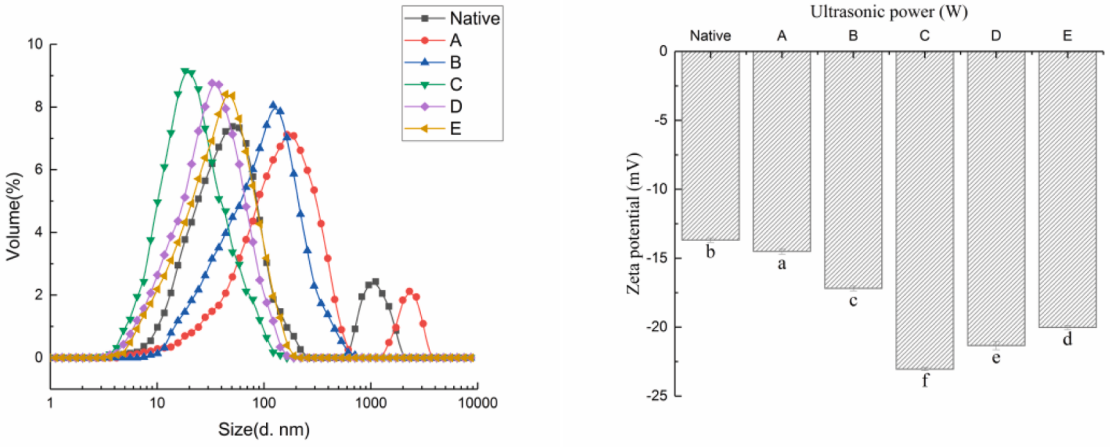

Fig. 3. Particle size and Zeta-potential of JRBP and JRBP-CC complex under different ultrasonic conditions. (a) Particle size. (b) Zeta-potential.

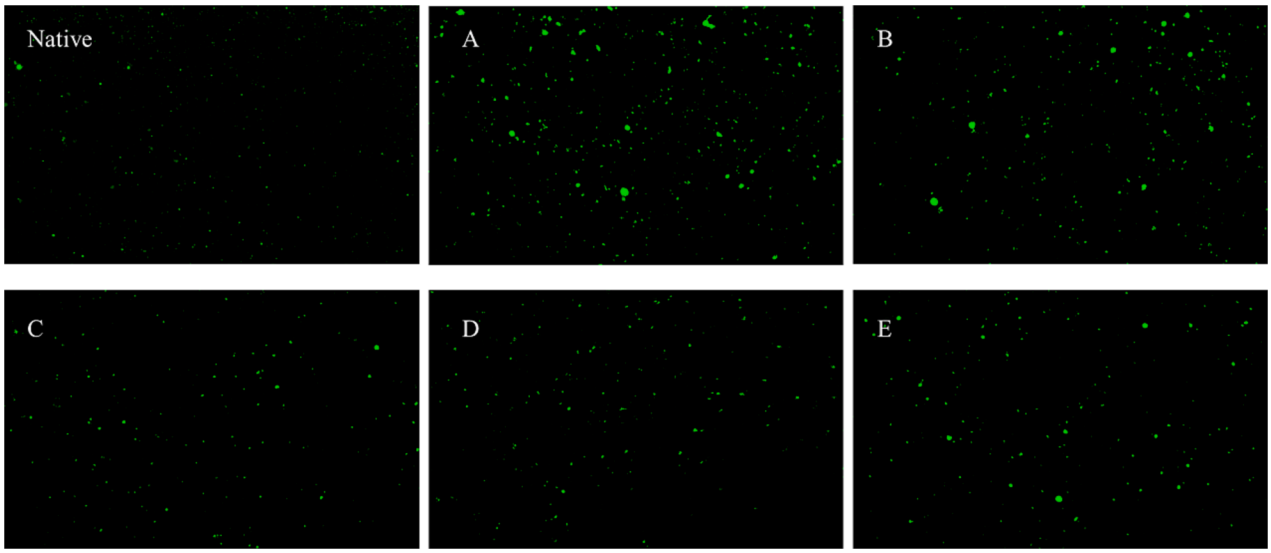

Fig. 4. Confocal laser scanning microscopy of JRBP and JRBP-CC complexes under different ultrasonic conditions.

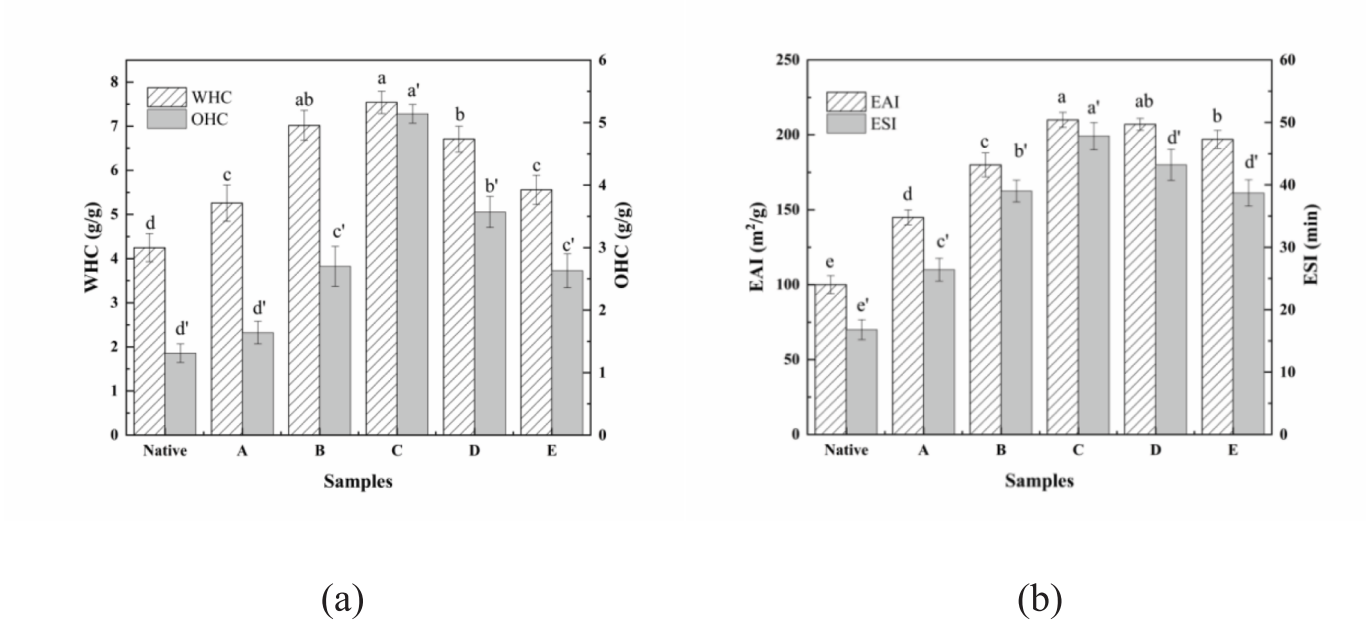

Fig. 5. Water holding capacity, oil holding capacity and emulsification of JRBP and JRBP-CC complexes under different ultrasonic conditions. (a)WHC and OHC. (b) Emulsifying properties.

side chains of JRBP, which in turn may cause changes in the hydrophobic/hydrophilic groups of JRBP, making it easier for JRBP and JRBP-CC to interact with water, leading to an increase in WHC. In addition, the OHC of JRBP and JRBP-CC showed a similar trend to that of WHC. Similarly, ultrasound treatment of JRBP can also change its spatial conformation, unfolding the protein structure, obtaining a larger specific surface area, and providing numerous lipophilic sites to bind more oil. Zhang et al. [44] suggested that the hydrophobic group was related to the change in OHC; Wu et al. [45] considered OHC to be closely associated with its own structure, especially the side chain groups and molecular size. This indicated that ultrasound improved the WHC and OHC of JRBP and JRBP-CC to some extent.

3.7. Emulsifying properties

The EAI and ESI of the samples were measured and the results are shown in Fig. 5(b). It can be seen from the figure that the EAI and ESI of JRBP were 100 m^2/g and 68.79 min, respectively. Compared with the IRBP prepared by Zhang et al. [43], JRBP had relatively better emulsification performance. Compared with the control group, the EAI and ESI of the JRBP-CC complexes increased by 45.0 % and 57.1 %, respectively (Sample B). The covalent bonding between CC and JRBP can be considered to have improved the emulsification properties. A similar situation occurred in the study of El-Maksoud et al. where covalent coupling of caffeic acid with β-lactoglobulin under alkaline conditions resulted in better emulsifying properties than natural lactoglobulin [46]. CC can change the surface properties of proteins, which not only improves the emulsification properties, but also facilitates the binding of polyphenols and proteins. Furthermore, the addition of CC would restrict protein movement, improve emulsion stability, and extend storage time [47]. Besides, changing the ultrasound power also resulted in the change of the EAI and ESI of the samples, both of which increased

with increasing ultrasound power at a lower power (<200 W), and the maximum value appeared at 200 W, when the EAI and ESI were 210 m^2/g and 47.8 min, respectively. The reason for this trend may be the turbulence and shear that ultrasound cavitation can generate. On the one hand, these forces temporarily dispersed or broke the non-covalent bonds maintaining the protein spatial structure, unfolding the protein structure. On the other hand, the smaller particle size of the samples formed by the above reasons would also favor rapid adsorption to the oil–water interface and promote the increase of the EAI and ESI values. Wang et al. discussed the influence of ultrasound on the functional properties of the rice bran protein-chlorogenic acid complex, and found that the emulsifying performance was the best when the ultrasound power was 200 W, indicating that cavitation induced protein unfolding and exposed the buried hydrophobic groups, thereby enhancing the emulsifying properties [17].

3.8. Antioxidant activity

3.8.1. Antioxidant activity of DPPH

The antioxidant capacity of the samples is shown in Table 3(a). CC was characterized by its high antioxidant activity because of its phenolic hydroxyl groups. In contrast, the antioxidant activity was relatively weak for proteins. The DPPH radical scavenging capacity of CC was as high as 86.76 %, whereas the value for JRBP was much lower (9.60 %). When complexation between CC and JRBP occurred through covalent interactions, the antioxidant activity of the JRBP-CC complexes was improved compared to the control. This phenomenon was mainly due to the covalent bonds formed between the side chains of JRBP and the aromatic rings of CC.

In addition, ultrasonic treatment of the complexes also altered the antioxidant properties of the samples. The DPPH radical scavenging rate of the complexes increased and then decreased with increasing ultrasound power. Among them, the DPPH radical scavenging rate of the JRBP-CC complex reached the maximum value of 71.96 % at the treatment power of 200 W. The increased antioxidant activity was probably explained by the following two factors: on the one hand, the ultrasonic waves produced bubble rupture, which to some extent unfolded the protein structure and promoted the covalent binding of JRBP to CC [48]. On the other hand, ultrasound induced exposure to antioxidant amino acids. This phenomenon was mainly due to the covalent bonds formed between the side chains of JRBP and the aromatic rings of CC. It has been shown that some amino acids produce protons that can react with free radicals and improve the antioxidant properties of JRBP-CC complexes [49].

3.8.2. Antioxidant activity of $ABTS^+$

The $ABTS^+$ scavenging ability of JRBP and samples under different ultrasound conditions are shown in the Table 3(b). As can be seen from the table, the $ABTS^+$ scavenging ability of CC was 90.31 %, while that of JRBP was relatively low (only 16.38 %). When CC was bound to JRBP, the $ABTS^+$ scavenging ability increased. This may be due to the covalent bonding between JRBP and CC, which improved the antioxidant activity of JRBP. In addition, the $ABTS^+$ scavenging ability first increased and then decreased with the increase of ultrasound power. When the ultrasound power was 200 W, the $ABTS^+$ scavenging ability of the JRBP-CC complex was 80.07 %, and that of the JRBP-CC complex increased by 8.29 % compared with that without ultrasound treatment. This further indicated that ultrasound treatment could improve the antioxidant activity of the JRBP-CC complex. Similar results were observed by Tong et al. [50], and the reason for this phenomenon may be the exposure of hydrophobic groups and hydrophobic amino acids of proteins after ultrasound treatment.

Table 3
Antioxidant activity of JRBP and JRBP-CC under different ultrasonic conditions.

Sample	(a) DPPH radical scavenging activity (%)	(b) $ABTS^+$ radical scavenging activity (%)
Catechin	86.76 ± 3.01^{a}	90.31 ± 2.71^{a}
Native	9.60 ± 2.56^{f}	16.38 ± 2.05^{g}
A	63.45 ± 2.71^{c}	71.78 ± 2.38^{b}
B	69.84 ± 1.54^{b}	76.49 ± 1.65^{c}
C	71.96 ± 1.71^{b}	80.07 ± 1.87^{d}
D	58.83 ± 1.32^{d}	74.83 ± 2.01^{e}
E	52.57 ± 1.48^{e}	68.38 ± 1.86^{f}

Note: The difference in letters indicates significant difference ($P < 0.05$).

4. Conclusions

In this paper, a JRBP-CC complex was prepared after ultrasound treatment of JRBP. The results showed that, compared with IRBP, the secondary structure of JRBP was very different, and it had a higher WHC content and better emulsification performance. After ultrasound processing, the secondary structure of the protein was gradually unfolded, and the particle size of JRBP-CC was small and well dispersed in the CLSM image. When the ultrasound power was 200 W, the λ_{max} of the JRBP-CC showed a redshift, the particle size was the smallest, the absolute value of the zeta potential was the largest, the hydrophobicity was the strongest, and the emulsification and oxidation resistance were the best. This discovery seeks to promote the application of JRBP-CC in the food industry to provide economic and social benefits.

CRediT authorship contribution statement

Yanfei Guo: Methodology, Investigation, Writing – original draft. **Minghao Wang:** Investigation, Validation, Data curation. **Kaiwen Xing:** Formal analysis. **Mingzhe Pan:** Supervision, Funding acquisition. **Liqi Wang:** Conceptualization, Writing – review & editing, Methodology, Supervision.

Declaration of Competing Interest

The authors declare that they have no known competing financial interests or personal relationships that could have appeared to influence the work reported in this paper.

Acknowledgment

This work was supported by a project from the “Hundred-Thousand-Ten Thousand” Engineering Science and Technology Major Special Project of Heilongjiang Province: Integration and demonstration of key technologies for soybean bio-based oil and protein products (No: 2020ZX08B01).

References

[1] A.A. Meharg, G. Norton, C. Deacon, P. Williams, E.E. Adomako, A. Price, Y. Zhu, G. Li, F.-J. Zhao, S. McGrath, A. Villada, A. Sommella, P.M.C.S. De Silva, H. Brammer, T. Dasgupta, M.R. Islam, Variation in rice cadmium related to human exposure, Environ. Sci. Tech. 47 (11) (2013) 5613–5618.

[2] T. Yoshihara, F. Goto, K. Shoji, Y. Kohno, Cross relationships of Cu, Fe, Zn, Mn, and Cd accumulations in common japonica and indica rice cultivars in Japan, Environ. Exp. Bot. 68 (2) (2010) 180–187, https://doi.org/10.1016/j.envexpbot.2009.10.006.

[3] D. Zhang, X. Duan, Y. Wang, B. Shang, H. Liu, H. Sun, Y. Wang, A comparative investigation on physicochemical properties, chemical composition, and in vitro antioxidant activities of rice bran oils from different japonica rice (Oryza sativa L.) varieties, J. Food Meas. Character. 15 (2021) 2064–2077, https://doi.org/10.1007/s11694-020-00806-5.

[4] D. Harriman, American association of textile chemists and colorists, Chem.. Heritage 24 (2) (2006) 27.

[5] D. Ph, H. Cheng, Total dietary fiber content of polished, brown and bran types of Japonica and Indica rice in Taiwan: Resulting physiological effects of consumption, Nutr. Res. 13 (1993) 93–101, https://doi.org/10.1016/s0271-5317(05)80660-8.

[6] N.-N. Wu, H.-H. Li, B. Tan, M. Zhang, Z.-G. Xiao, X.-H. Tian, X.-T. Zhai, M. Liu, Y.-X. Liu, L.-P. Wang, K. Gao, Free and bound phenolic profiles of the bran from

different rice varieties and their antioxidant activity and inhibitory effects on α-amylose and α-glucosidase, J. Cereal Sci. 82 (2018) 206–212.
[7] J. Qi, Y. Li, K.G. Masamba, C.F. Shoemaker, F. Zhong, H. Majeed, J. Ma, The effect of chemical treatment on the In vitro hypoglycemic properties of rice bran insoluble dietary fiber, Food Hydrocolloid. 52 (2016) 699–706, https://doi.org/10.1016/j.foodhyd.2015.08.008.
[8] F. Li, X. Wu, W. Wu, Effects of protein oxidation induced by rice bran rancidity on the structure and functionality of rice bran glutelin, LWT 149 (2021), 111874, https://doi.org/10.1016/j.lwt.2021.111874.
[9] C. He, Y. Hu, Y. Wang, Z. Liu, Y. Liao, H. Xiong, Q. Zhao, Design of water-soluble whole rice glutelin: The rendezvous of two ricCsubspecies, Japonica and Indica, Food Hydrocolloid. 110 (2021), 106148, https://doi.org/10.1016/j.foodhyd.2020.106148.
[10] P. Lai, K. Li, S. Lu, H. Chen, Phytochemicals and antioxidant properties of solvent extracts from Japonica rice bran, Food Chem. 117 (2009) 538–544, https://doi.org/10.1016/j.foodchem.2009.04.031.
[11] N. Wang, X. Zhou, W. Wang, L. Wang, L. Jiang, T. Liu, D. Yu, Effect of high intensity ultrasound on the structure and solubility of soy protein isolate-pectin complex, Ultrason. Sonochem. 80 (2021), 105808, https://doi.org/10.1016/j.ultsonch.2021.105808.
[12] Y. Meng, Z. Liang, C. Zhang, S. Hao, H. Han, P. Du, A. Li, H. Shao, C. Li, L. Liu, Ultrasonic modification of whey protein isolate: Implications for the structural and functional properties, LWT - Food Sci. Technol. 152 (2021), 112272, https://doi.org/10.1016/j.lwt.2021.112272.
[13] J. Chandrapala, C. Oliver, S. Kentish, M. Ashokkumar, Ultrasonics in food processing, Ultrason. Sonochem. 19 (2012) 975–983, https://doi.org/10.1016/j.ultsonch.2012.01.010.
[14] C.P. O'Donnell, B.K. Tiwari, P. Bourke, P.J. Cullen, Effect of ultrasonic processing on food enzymes of industrial importance, Trends Food Sci. Technol. 21 (7) (2010) 358–367.
[15] F. Xue, C. Zhu, F. Liu, S. Wang, H. Liu, C. Li, Effects of high-intensity ultrasound treatment on functional properties of plum, J. Sci. Food Agr. 98 (15) (2018) 5690–5699, https://doi.org/10.1002/jsfa.9116.
[16] L.H. Sun, F. Yu, Y.Y. Wang, S.W. Lv, L.Y. He, Effects of ultrasound extraction on the physicochemical and emulsifying properties of rice bran protein, Int. J. Food Eng. 17 (2021) 327–335, https://doi.org/10.1515/ijfe-2019-0115.
[17] T. Wang, X. Chen, W. Wang, L. Wang, L. Jiang, D. Yu, F. Xie, Effect of ultrasound on the properties of rice bran protein and its chlorogenic acid complex, Ultrason. Sonochem. 79 (2021), 105758, https://doi.org/10.1016/j.ultsonch.2021.105758.
[18] L. Jiang, J. Wang, Y. Li, Z. Wang, J. Liang, R. Wang, Y. Chen, W. Ma, B. Qi, M. Zhang, Effects of ultrasound on the structure and physical properties of black bean protein isolates, Food Res. Int. 62 (2014) 595–601, https://doi.org/10.1016/j.foodres.2014.04.022.
[19] D. Li, Y. Zhao, X. Wang, H. Tang, N. Wu, F. Wu, D. Yu, W. Elfalleh, Effects of (+)-catechin on a rice bran protein oil-in-water emulsion: Droplet size, zeta-potential, emulsifying properties, and rheological behavior, Food Hydrocolloid. 98 (2020), 105306, https://doi.org/10.1016/j.foodhyd.2019.105306.
[20] D. Karefyllakis, S. Salakou, J.H. Bitter, A.J. Vandergoot, C.V. Nikiforidis, Covalent bonding of chlorogenic acid induces structural modifications on sunflower proteins, ChemPhysChem 19 (2018) 459–468, https://doi.org/10.1002/cphc.201701054.
[21] Y.-R. Su, Y.-C. Tsai, C.-H. Hsu, A.-C. Chao, C.-W. Lin, M.-L. Tsai, F.-L. Mi, Effect of grape seed proanthocyanidin-gelatin colloidal complexes on stability and in vitro digestion of fish oil emulsions, J. Agr. Food Chem. 63 (46) (2015) 10200–10208.
[22] T.H. Quan, S. Benjakul, T. Sae-Leaw, A.K. Balange, S. Maqsood, Protein–polyphenol conjugates: Antioxidant property, functionalities and their applications, Trends Food Sci. Tech. 91 (2019) 507–517, https://doi.org/10.1016/j.tifs.2019.07.049.
[23] G.A. Tian, T.A. Dan, B. Cyha, R. Yu, H. Yong, Improving antioxidant ability of functional emulsifiers by conjugating polyphenols to sodium caseinate, LWT - Food Sci. Technol. 154 (2021), 112668, https://doi.org/10.1016/j.lwt.2021.112668.
[24] T. Wang, K. Chen, X. Zhang, Y. Yu, D. Yu, L. Jiang, L. Wang, Effect of ultrasound on the preparation of soy protein isolate-maltodextrin embedded hemp seed oil microcapsules and the establishment of oxidation kinetics models, Ultrason. Sonochem. 77 (2021), 105700, https://doi.org/10.1016/j.ultsonch.2021.105700.
[25] X. Sui, H. Sun, B. Qi, M. Zhang, Y. Li, L. Jiang, Functional and conformational changes to soy proteins accompanying anthocyanins: Focus on covalent and non-covalent interactions, Food Chem. 245 (2018) 871–878, https://doi.org/10.1016/j.foodchem.2017.11.090.
[26] G.L. Ellman, Tissue sulfhydryl groups, Arch. Biochem. Biophys. 82 (1959) 70–77, https://doi.org/10.1016/0003-9861(59)90090-6.
[27] I.M. Geremias-Andrade, N. Souki, I. Moraes, S.C. Pinho, Rheological and mechanical characterization of curcumin-loaded emulsion-filled gels produced with whey protein isolate and xanthan gum, LWT - Food Sci. Technol. 86 (2017) 166–173, https://doi.org/10.1016/j.lwt.2017.07.063.
[28] J. Li, J. Fu, Y. Ma, Y. He, R. Fu, A. Qayum, Z. Jiang, L. Wang, Low temperature extrusion promotes transglutaminase cross-linking of whey protein isolate and enhances its emulsifying properties and water holding capacity, Food Hydrocoll. 125 (2022) 107410.
[29] G. Zhu, Y. Li, L. Xie, H. Sun, Z. Zheng, F. Liu, Effects of enzymatic cross-linking combined with ultrasound on the oil adsorption capacity of chickpea protein, Food Chem. 383 (2022), 132641, https://doi.org/10.1016/j.foodchem.2022.132641.
[30] L. He, H. Xu, X. Liu, W. He, F. Yuan, Z. Hou, Y. Gao, Identification of phenolic compounds from pomegranate (Punica granatum L.) seed residues and investigation into their antioxidant capacities by HPLC–ABTS+ assay, Food Res. Int. 44 (2011) 1161–1167, https://doi.org/10.1016/j.foodres.2010.05.023.
[31] S.D. Zhou, Y.F. Lin, X. Xu, L. Meng, M.S. Dong, Effect of non-covalent and covalent complexation of (-)-epigallocatechin gallate with soybean protein isolate on protein structure and in vitro digestion characteristics, Food Chem. 309 (2020), 125718, https://doi.org/10.1016/j.foodchem.2019.125718.
[32] I. Hasni, P. Bourassa, S. Hamdani, G. Samson, R. Carpentier, H.A. Tajmir-Riahi, Interaction of milk α- and β-caseins with tea polyphenols, Food Chem. 126 (2011) 630–639, https://doi.org/10.1016/j.foodchem.2010.11.087.
[33] M. Shi, L. Huang, N. Nie, J. Ye, X. Zheng, J. Lu, Y. Liang, Binding of tea catechins to rice bran protein isolate: Interaction and protective effect during in vitro digestion, Food Res. Int. 93 (2017) 1–7, https://doi.org/10.1016/j.foodres.2017.01.006.
[34] Y. Meng, Z. Liang, C. Zhang, S. Hao, H. Han, P. Du, A. Li, H. Shao, C. Li, L. Liu, Ultrasonic modification of whey protein isolate: Implications for the structural and functional properties, LWT - Food Sci. Technol. 152 (2021), https://doi.org/10.1016/j.lwt.2021.112272.
[35] A. Handa, A. Gennadios, M.A. Hanna, C.L. Weller, N.J. Kuroda, Physical and molecular properties of egg-white lipid films, J. Food Sci. 64 (2010) 860–864, https://doi.org/10.1111/j.1365-2621.1999.tb15928.x.
[36] K. Zhang, Q. Wen, T. Li, Y. Wang, Y. Zhang, D. Luo, Comparative study of the effects of ultrasonic power on the structure and functional properties of gliadin in wheat and green wheat, J. Food Sci. 87 (3) (2022) 1020–1034.
[37] S. Ma, X. Yang, C. Zhao, M. Guo, Ultrasound-induced changes in structural and physicochemical properties of β-lactoglobulin, Food Sci. Nutr. 6 (2018) 1053–1064, https://doi.org/10.1002/fsn3.646.
[38] H. Xue, Y. Tu, G. Zhang, X. Xin, H. Hu, W. Qiu, D. Ruan, Y. Zhao, Mechanism of ultrasound and tea polyphenol assisted ultrasound modification of egg white protein gel, Ultrason. Sonochem. 81 (2021), 105857, https://doi.org/10.1016/j.ultsonch.2021.105857.
[39] M.M. Rahman, B. Byanju, D. Grewell, B.P. Lamsal, High-power sonication of soy proteins: hydroxyl radicals and their effects on protein structure, Ultrason. Sonochem. 64 (2020), 105019, https://doi.org/10.1016/j.ultsonch.2020.105019.
[40] S. Li, X. Yang, Y. Zhang, H. Ma, Q. Liang, W. Qu, R. He, C. Zhou, G.K. Mahunu, Effects of ultrasound and ultrasound assisted alkaline pretreatments on the enzymolysis and structural characteristics of rice protein, Ultrason. Sonochem. 31 (2016) 20–28, https://doi.org/10.1016/j.ultsonch.2015.11.019.
[41] C. Zhao, Z. Miao, J. Yan, J. Liu, Z. Chu, H. Yin, M. Zheng, J. Liu, Ultrasound-induced red bean protein–lutein interactions and their effects on physicochemical properties, antioxidant activities and digestion behaviors of complexes, LWT - Food Sci. Technol. 160 (2022), 113322, https://doi.org/10.1016/j.lwt.2022.113322.
[42] T.I. Li, X. Li, T. Dai, P. Hu, X. Niu, C. Liu, J. Chen, Binding mechanism and antioxidant capacity of selected phenolic acid-β-casein complexes, Food Res. Int. 129 (2020), 108802, https://doi.org/10.1016/j.foodres.2019.108802.
[43] H. Zhang, H. Zhang, L. Wang, X. Guo, Preparation and functional properties of rice bran proteins from heat-stabilized defatted rice bran, Food Res. Int. 47 (2012) 359–363, https://doi.org/10.1016/j.foodres.2011.08.014.
[44] S. Zhang, L. Zheng, X. Zheng, B. Ai, Y. Yang, Y. Pan, Z. Sheng, Effect of steam explosion treatments on the functional properties and structure of camellia (Camellia oleifera Abel.) seed cake protein, Food Hydrocoll. 93 (2019) 189–197.
[45] H. Wu, Q. Wang, T. Ma, J. Ren, Comparative studies on the functional properties of various protein concentrate preparations of peanut protein, Food Res. Int. 42 (2009) 343–348, https://doi.org/10.1016/j.foodres.2008.12.006.
[46] A.A.A. El-Maksoud, I.H.A. El-Ghany, H.S. El-Beltagi, S. Anankanbil, C. Banerjee, S. V. Petersen, B. Pérez, Z. Guo, Adding functionality to milk-based protein: Preparation, and physico-chemical characterization of β-lactoglobulin-phenolic conjugates, Food Chem. 241 (2018) 281, https://doi.org/10.1016/j.foodchem.2017.08.101.
[47] J. Zhao, W. Lv, J. Wang, J. Li, X. Liu, J. Zhu, Effects of tea polyphenols on the post-mortem integrity of large yellow croaker (Pseudosciaena crocea) fillet proteins, Food Chem. 141 (2013) 2666–2674, https://doi.org/10.1016/j.foodchem.2013.04.126.
[48] J. Jiang, B. Zhu, Y. Liu, Y.L. Xiong, Interfacial structural role of pH-shifting processed pea protein in the oxidative stability of oil/water emulsions, J. Agr. Food Chem. 62 (7) (2014) 1683–1691.
[49] D. Stanic-Vucinic, I. Prodic, D. Apostolovic, M. Nikolic, T.C. Velickovic, Structure and antioxidant activity of β-lactoglobulin-glycoconjugates obtained by high-intensity-ultrasound-induced Maillard reaction in aqueous model systems under neutral conditions, Food Chem. 138 (2013) 590–599, https://doi.org/10.1016/j.foodchem.2012.10.087.
[50] X. Tong, J. Cao, T. Tian, B. Lyu, L. Miao, Z. Lian, W. Cui, S. Liu, H. Wang, L. Jiang, Changes in structure, rheological property and antioxidant activity of soy protein isolate fibrils by ultrasound pretreatment and EGCG, Food Hydrocolloid. 122 (2022), 107084, https://doi.org/10.1016/j.foodhyd.2021.107084.